Solid Earth Discuss., 6, 1–30, 2015
www.solid-earth-discuss.net/6/1/2015/
doi:10.5194/sed-6-1-2015

Solid Earth Discussions
Open Access

Effects of vegetation restoration on the aggregate stability and distribution of aggregate-associated organic carbon in a typical karst gorge region

F. K. Tang[1], M. Cui[1], Q. Lu[1], Y. G. Liu[1], H. Y. Guo[2], and J. X. Zhou[2]

[1]Institute of Desertification Studies, Chinese Academy of Forestry, Beijing, China
[2]Beijing Forestry University, Key Laboratory of Soil and Water Conservation and Desertification Combating, Ministry of Education, Beijing, China

Received: 27 June 2015 – Accepted: 7 July 2015 – Published:

Correspondence to: M. Cui (cuiming2009@foxmail.com)

Published by Copernicus Publications on behalf of the European Geosciences Union.

Abstract

Changes in soil utilization significantly affect aggregate stability and aggregate-associated soil organic carbon (SOC). A field investigation and indoor analysis were conducted in order to study the soil aggregate stability and organic carbon distribution in the water-stable aggregates (WSA) of the bare land (BL), grassland (GL), shrubland (SL), and woodland (WL) in a typical karst gorge region. The results indicated that the BL, GL, SL, and WL were dominated by particles with sizes > 5 mm under dry sieving treatment, and that the soil aggregate contents of various sizes decreased as the particle size decreased. In addition, the BL, GL, SL, and WL were predominantly comprised of WSA < 0.25 mm under wet sieving treatment, and that the WSA contents initially increased, then decreased, and then increased again as the particle size decreased. Furthermore, at a soil depth of 0–60 cm, the mean weight diameter (MWD), geometrical mean diameter (GMD), and fractal dimensions (D) of the dry aggregates and water-stable aggregates in the different types of land were ranked, in descending order, as WL > GL > SL > BL. The contents of WSA > 0.25 mm, MWD and GMD increased significantly, in that order, and the percentage of aggregate destruction (PAD) and fractal dimensions decreased significantly as the soil aggregate stability improved. The results of this study indicated that, as the SOC contents increased after vegetation restoration, the average SOC content of WL was 2.35, 1.37, and 1.26 times greater than that in the BL, GL, and SL, respectively. The total SOC and SOC associated in WSA of various sizes were the highest at a soil depth of 0–20 cm. In addition, the SOC contents of the WSA increased as the soil aggregate sizes decreased. The SOC contents of the WSA < 0.25 mm were highest except in the bare land, and the SOC contents of the aggregates < 0.25 mm, which ranged from 18.85 to 41.08 %, comprised the majority of the total aggregate SOC contents. The woodland and grassland facilitated WSA stability and SOC protection, thus, promoting the natural restoration of vegetation by reducing artificial disturbances could effectively restore the ecology of and prevent soil erosion in karst regions.

1 Introduction

Soil aggregates, the basic units of soil structures, act as carriers in the stabilization and protection of organic carbon. Good soil structures provide solid foundations for the storage and stabilization of organic carbon (Jastrow, 1996; Mao et al., 2007). The particle sizes of aggregates affect their abilities to store organic carbon as well as the distributions of their stored organic carbon components (Abu-Hamdeh et al., 2005; Liu et al., 2009). The particle sizes distribution and stability of soil aggregates are closely related to the erosion resistance of soil and, thereby, are effective indicators of erosion sensitivity (Guo et al., 2007; Rachman et al., 2003; Valmis et al., 2005). The results of studies conducted by Le Bissonnais (1996, 1997) indicated that soil erosion primarily result from the destruction of soil aggregates. Young (1980) and Bryan (2000) determined that aggregate stability affects the erodibility and nutrient holding capacity of soil. The formation and stability of the water-stable aggregates in soil are dependent on soil organic carbon (SOC). Recent studies have primarily focused on the effects of changes in land use on the stability and distribution of organic carbon in soil aggregates (Jastrow, 1996; Unger, 1997).

China's karst region comprises an area of 3.44×10^6 km^2. The ecosystems that have developed from the karst landforms in this region are characterized by simple ecological community structures, small environmental capacities, and weak resistance to interference. These ecologically vulnerable areas typical to china are subjected to significant land degradation and stony desertification (Yuan et al., 2002). The SOC pool is the largest carbon pool in the karst system (Pan and Cao, 1999); the transfer of carbon in the karst system is predominantly controlled by soil carbon. Excessive land utilization and management often result in the destruction of soil structures, the disturbance of the foundations for organic carbon sequestration, the acceleration of soil carbon pool activity, and increased levels of soil erosion (Tang et al., 2014). Previous studies concerning the stability of soil aggregates and the characteristics of the organic carbon in those aggregates have primarily been conducted in the Loess Plateau (Liu

SED
6, 1–30, 2015

et al., 2013; Qi et al., 2011) and hilly red soil regions (Guo et al., 2007; Yan et al., 2007). Studies regarding the karst region have only recently been conducted. Due to strong karstification, the karst region possesses a unique surface-underground structure and soil erosion different from that in the Loess Plateau and hilly red soil regions, showing that soil leakage underground occurs in addition to soil erosion on the surface (Zhang et al., 2011). Previous studies concerning the distribution of the soil aggregates, aggregate stability, and distribution and mineralization of the organic carbon in the aggregates (Wei et al., 2011; Tan et al., 2014) of the karst region have primarily consisted of single-factor studies. In addition, due to the differences in surface vegetation, litter, and roots resulting from the strong spatial heterogeneity of karst soil, the properties of the soil in different regions vary importantly. Previous studies have failed to determine the relationship between the soil structures and soil depth in the karst region (Li et al., 2013). Therefore, the effects of vegetation restoration efforts on the aggregate stability and organic carbon distributions of various karst ecosystems require further investigation.

In this paper, the effects of vegetation restoration on the stability of the soil aggregates and the distribution and accumulation of the organic carbon in the aggregates in the karst region were analyzed by studying grassland (GL), shrubland (SL), woodland (WL), and bare land (BL) soil typical to the gorge region of the karst plateau in Guizhou Province, China. Furthermore, the influencing mechanism of vegetation restoration on the stability of soil structures and sequestration of organic carbon were investigated in order to provide a scientific basis for future studies regarding the changes in the carbon source/sink functions of the soil in the karst region and provide a reference concerning the restoration and reconstruction of degenerated karst ecosystems.

2 Materials and methods

2.1 Study area

The study area was located in the Huajiang Gorge (25°40′–25°42′ N, 105°37′–105°39′ E) demonstration area of Guanling County in Guizhou Province, China. This area, located on the eastern slope of the Yunnan–Guizhou Plateau tilting toward the hills in Guangxi, is a typical gorge region on the karst plateau, with an altitude of 500–1200 m and a relative height difference of 700 m. This region is characterized by a mid-subtropical humid monsoon climate, with sufficient heat, an annual average temperature of approximately 18 °C, and an average annual rainfall of 1200 mm. The typical soils in this area are Calcaric Leptosols according to WRB-based soil classification, which are badly structured, dry and barren.

The zonal vegetation in this area is comprised of mid-subtropical broadleaved evergreen forests. Due to the influence of several factors, such as lithology, drought, soil, and human activity, this area has experienced significant levels of vegetative degradation and is characterized by fragile ecosystems and a small environmental carrying capacity. The arbor forests, shrubs, and herbs in this region primarily consist of *Pteroceltis tatarinowii*, *Tona sinensis*, and *Sapium sebiferum*; *Pyracantha fortuneana*, *Dodonaea viscosa*, *Zanthoxylum bungeanum*, and *Rosa cymosa*; and *Imperata cylindrica*, *Arthraxon hispidus*, *Taraxacum mongolicum*, and *Dicranopteris dichotoma*, respectively. Four types of vegetation typical to this area, including bare land (BL), grassland (GL), shrubland (SL) and woodland (WL) were selected for the purposes of this study through field vegetation and soil investigations. The characteristics of the sample plots are shown in Table 1.

2.2 Sample collection and analysis

Three 20 m × 20 m standard sample plots were established for each vegetation type in August 2012. Sampling points were defined in the form of quincunxes within the sample plots. Soil samples were collected at depths of 0–20, 20–40, and 40–60 cm while leaving the soil undisturbed. A total of thirty-six soil samples were collected for the purposes of the study. The samples were brought indoors, broken into 10 mm clods along their soil cracks, and air-dried indoors.

The water stability of the soil aggregates was determined using the conventional wet-sieving method proposed by н.и. Саввинов. This method was used to identify the disintegration processes of the soil aggregates under dissipation and expansion (Qi et al., 2011). First, the air-dried soil samples were mixed well, and approximately 1 kg of soil samples was obtained by quartering and sieving the samples with sieves with mesh sizes of 8, 5, 2, 1, 0.5, and 0.25 mm. Then, a total of 100 g of the dry-sieved aggregates with different size fractions was weighed and placed on sieves with mesh sizes of 5, 2, 1, 0.5, and 0.25 mm. The soil samples became saturated after being wet for 10 min. The soil samples were shaken vertically for five minutes at an amplitude of 3 cm and a frequency of 30 times min^{-1}. Then, the residue on the sieves was collected, dried at 60 °C, and weighed (Sainju et al., 2003). The total SOC and SOC associated in water-stable aggregates were determined through oxidation with potassium dichromate and external heating (Bao, 2005).

2.3 Data calculation and analysis

The contribution rate of aggregates to SOC (y) were calculated using Eq. (1):

$$y = x_1 \times \frac{x_2}{w} \times 100\,\%, \qquad (1)$$

where x_1 = percent of aggregates in this size fraction (%); x_2 = content of SOC associated in aggregates ($g\,kg^{-1}$); w = contents of total organic carbon in soil ($g\,kg^{-1}$).

SED
6, 1–30, 2015

The transfer matrix method proposed by Shi (2005) was used to evaluate the aggregate stability index (ASI). The basic equations are:

$$\mathbf{M}_i X_i = \mathbf{N}_i \quad (2)$$

$$\text{ASI} = X_1 + X_2 + X_3 + \ldots + X_i, \quad (3)$$

where $\mathbf{M}_i$ = matrix TS2 of dry-sieved aggregates contents in i particle size ranges; $\mathbf{N}_i$ = matrix of wet-sieved aggregates contents in i particle size ranges; X_i = the probability that each aggregate size would remain unchanged.

The percentage of aggregate destruction (PAD) was expressed as:

$$\text{PAD} = \frac{w_1 - w_2}{w_1} \times 100\,\%, \quad (4)$$

where w_1 = contents of dry-sieved aggregates > 0.25 mm (%); w_2 = contents of water-stable aggregates > 0.25 mm (%).

The mean weight diameter (MMD) and geometrical mean diameter (GMD) of the aggregates were calculated as (Yan et al., 2007; He et al., 2011):

$$\text{MMD} = \sum_{i=1}^{n} x_i w_i \quad (5)$$

$$\text{GMD} = \exp\left[\sum_{i=1}^{n} w_i \ln x_i \Big/ \sum_{i=1}^{n} w_i\right], \quad (6)$$

where x_i = the average particle size of two adjacent aggregate size fractions during sieving (mm); w_i = the mass percentage of the aggregates in the i size fraction (%); $\ln x_i$ = the natural logarithm of the average diameter of the soil particle sizes.

Also, the fractal dimension (D) of the aggregates was calculated using the fractal model of soil, in which the weight distribution of soil particle sizes characterizes the quantity distribution (Tyler and Wheatcraft, 1989; Yang et al., 1993):

$$D = 3 - \frac{\log(W_i/W_0)}{\log(\overline{d_i}/d_{max})}, \quad (7)$$

where $\overline{d_i}$ = the average particle size of two sieve fractions (d_i and d_{i-1}, mm); d_{max} = the average maximum particle size (mm); W_i = the cumulative content of the soil particles ($> d_i$, %); W_0 = the sum of the soil weight with various particle sizes (%).

In this study, all of the data was analyzed using Excel 2003 and SPSS 18.0. The data conforms to normal distribution upon examination. The one-way analysis of variance (one-way ANOVA) and least significant difference (LSD) values were used to compare the differences among the various data sets. Pearson's correlation coefficient was used to evaluate the correlations among the different factors. The significance level was defined as $\alpha = 0.05$.

3 Results

3.1 Soil aggregates relative distribution

As shown in Fig. 1, the constituent size fractions of the dry-sieved aggregates in the different types of vegetation differed. For all vegetation types, the dry-sieved aggregates in the different layers of soil predominantly consisted of aggregates ≥ 2 mm, accounting for greater than 60 % of the total aggregates. The aggregates > 5 mm also comprised a large amount of the soil aggregates, accounting for 35.56–60.98 % of the total aggregates. The aggregates < 0.25 mm comprised the smallest proportion of aggregates, accounting for 3.52–8.49 % of the total aggregates. In general, the aggregate contents decreased as the particle size decreased. Each size fraction of the soil aggregate contents varied among the different types of vegetation, but not importantly. The soil aggregate contents of different size fractions varied somewhat within each type of vegetation.

For all four vegetation types, the contents of the aggregates > 5 mm decreased as the soil depth increased, the contents of the aggregates < 0.25 mm increased as the soil depth increased, and the contents of the aggregates with other particle sizes varied differently as the soil depth varied. Within the various layers of soil, the contents of the aggregates > 5 mm were ranked, in descending order, as WL > GL > SL > BL, and the contents of the aggregates ranging from 2 to 5 mm were ranked, in descending order, as SL > BL > GL > WL. The contents of the aggregates < 0.25 mm in the top soil decreased as the vegetation restoration progressed.

As shown in Fig. 2, the WSA of the different types of vegetation predominantly consisted of particles with sizes < 0.25, 1–2, and 2–5 mm, accounting for 59.01–71.31 % of the total WSA. In general, the WSA contents initially increased, then decreased, and then increased as the particle sizes decreased. The WSA < 0.25 mm comprised the majority of the total WSA, accounting for 23.64–35.93 % of the total WSA. Within the various layers of soil, the content of aggregates < 0.25 mm in the different types of vegetation increased as the soil depth increased according to the ranking BL > SL > GL > WL, while the contents of the larger aggregates decreased as the soil depth increased. The BL exhibited the highest content of aggregates < 0.25 mm in the various layers of soil. The contents of aggregates < 0.25 mm in the other vegetation types were less than 30 %.

3.2 Soil aggregate stability

As shown in Table 2, the stability of the soil aggregates differed significantly based on the type of vegetation. The soil depth also affected the stability of the soil aggregates. The contents of the aggregates > 0.25 mm in the WL, GL, SL, and BL, in descending order, were equal to 81.37, 79.49, 69.02, and 68.65 %, respectively. The PAD of the aggregates > 0.25 mm in the BL (27.24 %) was the highest, and the PAD of the aggregates > 0.25 mm in the WL (16.27 %) was the lowest. The MWD and GMD values of the different types of vegetation varied consistently. The MWD and GMD values of the wet- and dry-sieved aggregates were both ranked, in descending order, as

WL > GL > SL > BL. The D values of the dry-sieved aggregates in the four types of vegetation ranged from 1.994 to 2.227, and the D values of the WSA ranged from 2.425 to 2.725, ranking, in descending order, as BL > SL > GL > WL at a soil depth of 0–60 cm.

In all four types of vegetation, the contents of the aggregates > 0.25 mm, MWD and GMDs decreased as the soil depth increased. In addition, the PAD and D values increased as the soil depth increased. The MWD and GMD of the dry-sieved and wet-sieved aggregates in the various layers of soil were ranked, in descending order, as WL > GL > SL > BL, while the D values of the dry- and wet-sieved aggregates in the various layers of soil were ranked, in descending order, as BL > SL > GL > WL. The PADs of the aggregates obtained at a soil depth of 0–20 cm were ranked, in descending order, as SL > BL > GL > WL, while the PADs of the aggregates obtained at soil depths of 20–40 and 40–60 cm were ranked, in descending order, as BL > SL > WL > GL. The stability of the soil aggregates in the same soil layers of the different types of vegetation varied significantly ($P < 0.05$). Other indicators changed not significantly as the soil depth changed.

The probabilities of the soil aggregates in the different types of vegetation remaining unchanged are shown in Table 3. In the BL, GL, and SL, dry- and wet-sieving essentially destroyed the aggregates with particle sizes greater than 5 mm and ranging from 1 to 5 mm, and somewhat affected the aggregates with sizes ranging from 0.25 to 1 mm. The probability of the soil aggregates with sizes ranging from 0.25 to 1 mm remaining unchanged ranged from 0.26 and 0.51. In the WL soil, the probability of the soil aggregates > 5 mm remaining unchanged was the highest (0.39–0.55), and the probability of the soil aggregates with sizes ranging from 0.25 to 0.5 mm only ranged from 0.23 to 0.31, indicating that these particles were easily broken when subjected to dissipation and disintegration. The ASI values varied significantly, ranging from 2.19 to 3.32. The average ASI values of the WL, GL, SL, and BL were, in descending order, equal to 2.85, 2.65, 2.39, and 2.31, respectively. The ASI values of the aggregates in the topsoil were the highest, and the ASI values decreased as the soil depth increased. The ASI values of the different types of vegetation at various soil depths were ranked, in descending order, as WL > GL > SL > BL. The differences in the ASI values of the GL and WL, as well as BL and SL at the same soil depths were not significant. However, except at soil depths of 20–40 cm and 40–60 cm, the differences in the ASI values of the GL and BL and the WL and SL at the same soil depths were significant.

3.3 Distribution of the organic carbon in water-stable aggregates

The SOC contents of soil aggregates with various particle sizes can be used to micro-characterize the balance between organic matter and the mineralization rate of organic carbon. Thus, these contents significantly affect the soil fertility and carbon sinks of soil. As shown in Fig. 3, the organic carbon contents of the aggregates with various particle sizes differed significantly based on the type of vegetation. The total organic carbon content of the study area ranged from 10.25 to 34.07 $g\,kg^{-1}$. The organic carbon contents of the soil in the WL, SL, GL, and BL were highest at a soil depth of 0–20 cm and decreased as the soil depth increased. The total organic carbon contents of the various soil layers were ranked, in descending order, as WL > SL > GL > BL.

The organic carbon contents of the aggregates with different size fractions differed, though not significantly, based on the type of vegetation. In the BL, at a soil depth of 0–40 cm, the organic carbon contents of the aggregates with sizes of 0.5–1 and 0.25–0.5 mm were the highest; at a soil depth of 40–60 cm, the organic carbon content of the aggregates < 0.25 mm was highest. However, this difference was not significant ($P > 0.05$). In the GL, SL, and WL, the contents of the aggregates < 0.25 mm were the highest. In general, the organic carbon content decreased as the particle size increased. In addition, the organic carbon content of the aggregates > 5 mm was the lowest and differed significantly from those of the aggregates with different particle sizes, indicating that the organic carbon in the WSA with larger particle sizes exhibited more sensitive responses to forest restoration.

The organic carbon contents of the soil aggregates with various sizes were highest in the topsoil. In the BL, the organic carbon contents of the aggregates with particle sizes of > 5, 1–2, and 0.25–0.5 mm initially decreased, then increased as the soil depth in-

SED
6, 1–30, 2015

creased, and the organic carbon contents of the aggregates with other size fractions decreased as the soil depth increased. In the SL, the organic carbon contents of the aggregates with particle sizes of 0.25–0.5 and < 0.25 mm initially decreased, then increased as the soil depth increased, and the organic carbon contents of the aggregates with other particle sizes decreased as the soil depth increased. In the GL and WL, the organic carbon contents of the soil aggregates with various size fractions decreased as the soil depth increased.

As shown in Table 4, in all of the types of vegetation, the contribution of the organic carbon in the $WSA_{<0.25\,mm}$ to the total organic carbon content of the soil was highest, ranging from 18.85 and 41.08 %, with an average of 25.95 %. In the BL, GL, and SL, the contribution of the organic carbon contents of the aggregates > 5 mm was lowest with values of less than 10 %. In the WL, the contribution of the organic carbon contents of the WSA with sizes of 0.25–0.5 mm was the lowest. At different soil depths, the contributions of the organic carbon contents of the WSA with various sizes to the total organic carbon contents of the aggregates varied insignificantly.

3.4 Relationships between water stable aggregates and organic carbon

The correlations among the parameters of the WSA are shown in Table 5. D was significantly and negatively associated with the MWD, GMD, and SOC ($P < 0.01$), and the MWD was significantly and positively associated with the GMD ($P < 0.01$). The SOC was significantly and positively associated with both the MWD and GMD ($P < 0.01$), indicating that, as the SOC increased, the MWD and GMD also increased, promoting the stability of the soil structures. The contents of the aggregates with particle sizes of greater than 5, 2–5, and 1–2 mm were significantly and negatively correlated with D ($P < 0.05$), and the contents of the aggregates with particle sizes of 0.25–0.5 and less than 0.25 mm were significantly and positively correlated with D ($P < 0.05$). The MWD and GMD were significantly and positively correlated with the contents of the aggregates > 2 mm and significantly and negatively correlated with the contents of the aggregates < 0.5 mm. The SOC was positively correlated with the contents of

SED
6, 1–30, 2015

aggregates with various size fractions and significantly correlated with the contents of aggregates greater than 5 mm, indicating that, as the content of soil aggregates with large size fractions increased, the stability of the soil structures and the levels of soil organic carbon increased.

4 Discussion

4.1 Effects of vegetation restoration on the distribution and stability of soil aggregates

The size fractions of aggregates affect the storage and supply of soil nutrients, the pore structure and hydraulic properties of soil, and the movement of organisms in soil. Therefore, the size distributions of aggregates are closely related to soil quality (Dexter, 1988; Nimmo and Perkins, 2002). Soil organic carbon is a binding substance imperative for the formation of aggregate structures (Wu et al., 2004). Land utilization significantly affects soil organic carbon contents by influencing the input and output of the organic matter in soil and, thereby, the distribution and stability of soil aggregates (Luo et al., 2011). After vegetation restoration, the organic carbon contents, MWD, and GMD of the WSA > 0.25 mm increased, and the PAD and *D* values decreased. Thus, as a result of vegetation restoration, the soil organic carbon content increased, promoting the formation of soil aggregates and increasing the stability of the soil aggregates. The organic carbon contents, MWD, and GMD of the WSA > 0.25 mm in the WL and GL were significantly higher than those of the WSA > 0.25 mm in the BL and SL, while the PAD values of the WL and GL were significantly lower than those of the BL and SL, indicating that the WL and GL possessed good soil aggregate structures with strong corrosion resistance and high nutrient storage capacities. In the BL and SL, artificial disturbances led to the destruction of soil structures, accelerating the transformation of large WSA to aggregates with small size fractions and exacerbating the low of soil and nutrients. The structural stability and erosion resistance of the soil in the GL were

SED
6, 1–30, 2015

higher than those of the soil in the SL, primarily because the GL was subjected to less artificial disturbances. Thus, the GL exhibited higher levels of vegetative coverage with considerable amounts of returned biomass, while the SL, due to felling, picking, and the forced compaction of wildlife, possessed fewer soil organic matter sources and disrupted soil structures.

The contents of the WSA decreased as the soil depth increased. This was likely because the excess litter on the topsoil; the high organic matter contents; and the good water, heat, and air conditions of the soil contributed to the formation of large aggregates (Tisdall and Oades, 1982; Xiao et al., 2008). In addition, the organic matter contents of the deep soil were relatively low, a small number of large soil aggregates were formed, and the contents of the large WSA were reduced. In the same types of vegetation, the ASI of the WSA decreased as the soil depth increased, just as the contents of the large WSA decreased as the soil depth increased. Of the four typical types of vegetation in the study area, the WL exhibited the highest aggregate stability and strongest erosion resistance, promoting the stability of the soil structures, the storage of nutrients, and the contents of organic carbon. The grassland exhibited the second highest aggregate stability, and the bare land and shrubland possessed relatively poor water stability.

The vegetation restoration process significantly affected the formation and distribution of large aggregates in that the BL, SL, GL, and WL exhibited significantly decreased levels of aggregates < 0.25 mm throughout the various soil layers and significantly increased levels of larger aggregates throughout the vegetation restoration process. Thus, vegetation restoration effectively improved the soil infiltration capacity, water holding capacity, and aeration of the lime soils. Therefore, aggregate stability could be improved and soil erosion could be prevented by reducing artificial disturbances, increasing the organic matter and nutrient contents of soil, and, thereby, facilitating the natural restoration of vegetation.

4.2 Fractal characteristics of the aggregates and their responses to vegetation restoration

The size fractions of aggregates affect the storage and supply of soil nutrients, the pore structure and hydraulic properties of soil, and the movement of organisms in soil. The fractal dimensions of the particle size distributions of soil granular structures reflect the influence of the contents of aggregates on the structure and stability of the soil (Dexter, 1988; Nimmo and Perkins, 2002). Thus, smaller fractal dimensions indicate better soil structures and stability and higher erosion resistance. Likewise, higher fractal dimensions indicate poorer soil structures and stability (Zhou et al., 2008; Barral et al.,1998). In this study, the fractal dimensions of the dry-sieved soil aggregates in the four types of vegetation varied insignificantly from 1.994 to 2.227. In the BL, the fractal dimensions of the soil aggregates at soil depths of 40–60 cm were the highest. In the WL, the fractal dimensions of the soil aggregates in the top soil (0–20 cm) were the lowest. The fractal dimensions of the WSA ranged from 2.425 to 2.725. In all of the vegetation types, the fractal dimensions of the dry-sieved soil aggregates were significantly less than those of the wet-sieved soil aggregates by 0.414–0.531. The fractal dimensions of the WSA in the topsoil (0–20 cm) of the GL, SL, and WL were 0.162, 0.046, and 0.224 less than that of the BL, respectively. The fractal dimensions of the soil aggregates in the GL, SL, and WL at a soil depth of 20–40 cm were 0.185, 0.067, and 0.168 less than that of the BL, respectively. Furthermore, the fractal dimensions of the soil aggregates in the GL, SL, and WL at a soil depth of 40–60 cm were 0.145, 0.047, and 0.169 less than that of the BL, respectively. These results indicated that, as the vegetation was restored, the fractal dimensions of the WSA decreased. The fractal dimensions of the mechanically stable soil aggregates and WSA in all of the types of vegetation increased as the soil depth increased, but the fractal dimensions at different soil depths varied insignificantly ($P > 0.05$).

The fractal dimensions of the mechanically stable aggregates in the different types of vegetation exhibited no significant differences (Table 2). The fractal dimensions of the

SED
6, 1–30, 2015

mechanically stable aggregates in the BL were the highest, and the fractal dimensions of the mechanically stable aggregates in the WL were the lowest, indicating that the amount of soil aggregation in the WL was highest. This could have been because the lack of artificial disturbances and low structural dispersion of the WL over long periods of time facilitated soil aggregation improvements. Furthermore, the significant artificial disturbances in the other types of vegetation could have resulted in the destruction of soil aggregates. The fractal dimensions of the WSA in the GL and WL were not significantly different, while the fractal dimensions of the WSA in the BL and SL, GL and BL, and WL and SL were significantly different. The fractal dimensions of the WSA in the various types of vegetation were ranked, in descending order, as BL > SL > GL > WL. The fractal dimensions of the BL were the highest, and the fractal dimensions of the WL were the lowest, indicating that the artificial disturbances affected the soil stability of the BL most significantly, and that the stability of the WL was the highest.

The fractal dimensions of various soil particle sizes reflect the ability of the soil particles to fill spaces and could be used to evaluate soil structures (Tyler and Wheatcraft, 1989; Yang et al., 1993). D was significantly and negatively correlated with the MWD, GMD, and SOC, indicating that, as the value of D increased, the contents of the aggregates > 0.25 mm decreased, and the soil density increased, resulting in poorer permeability and nutrient and moisture storage capacities. The results of this study indicated that, as the vegetation was restored, the fractal dimensions of the WSA decreased, and the stability of the soil structures and organic carbon contents improved.

4.3 Effects of vegetation restoration types on distribution of SOC associated in water-stable aggregates

The organic carbon contents of aggregates, which reflect the balance and mineralization of organic carbon, significantly affect the nutrient holding capacity and carbon sequestration in soil (Wu et al., 2004). The humus horizons of the various types of vegetation differed based on the quantity and quality of the litter and the environment, affecting the organic carbon contents of the soil and the stability and contents of the organic carbon in the aggregates (Novara et al., 2015). In all four types of vegetation, the organic carbon contents in the aggregates with various particle sizes were the highest at a soil depth of 0–20 cm. These results were consistent with the results of a study conducted by Li et al. (2008). This was because the large amount of plant residue that had accumulated in the topsoil and the amount of organic matter that had been input into the soil improved the biological activity of the microorganisms, animals, and roots in the topsoil and, thus, facilitated the formation of particulate organic carbon (Wei et al., 2011).

In this study, as the vegetation transitioned from BL to WL, the total soil organic carbon contents and the organic carbon contents in the aggregates with various particle sizes increased significantly. The organic carbon contents of the aggregates were the highest in the WL, and the lowest in the SL and BL, primarily due to the amount of vegetative coverage and the quantity and decomposition of litter. Due to their high amounts of vegetative coverage, the WL and GL exhibited large amounts of litter and a considerable amount of input soil organic carbon. The BL and SL exhibited significantly smaller amounts of litter and input soil organic carbon and accelerated levels of organic carbon decomposition due to artificial disturbances. In general, the organic carbon contents of the soil aggregates decreased as the soil depth increased; in these types of vegetation, artificial disturbances accelerated the decomposition of organic carbon.

In previous studies, De Jonge (1999), Christensen (1986), and Li et al. (2006) determined that organic carbon is primarily distributed in micro-aggregates (< 0.25 mm) and that organic carbon contents increase as aggregate particle sizes decrease. Puget (1998, 2000) found that large aggregates are a source of organic carbon enrichment. In another study, Li et al. (2000) found that organic carbon is distributed in a "V" shape in aggregates and that the organic carbon contents of aggregates > 2 and < 0. 25 mm are high. In Li's study, as the particle sizes increased, the soil organic carbon contents decreased, but the organic carbon contents of the aggregates exhibited no significant differences, possibly due to the high calcium carbonate and clay contents of the lime soil in the karst region (Wei et al., 2011). In this study, the organic carbon contents of the aggregates < 0.25 mm in the grassland, shrubland, and woodland increased by 5.28–95.37, 1.46–106.25, and 6.02–85.43 % compared to the aggregates with other particle sizes. These results corresponded with the theory that organic carbon initially accumulates in aggregates with small size fractions (Hassink, 1997) as well as the results of other studies concerning the karst region (Lu et al., 2012; Luo et al., 2011).

5 Conclusions

As a result of the vegetation restoration of bare land to woodland on the Karst Plateau, the content of WSA < 0.25 mm decreased significantly, and the content of WSA > 1 mm increased, contributing to the accumulation of aggregates with small particle sizes into aggregates with large particle sizes and, thereby, improving the water stability of soil. Fractal dimensions of aggregates could be used to objectively and comprehensively reflect the aggregate characteristics and stability of soil. The fractal dimensions of water-stable aggregates in this study was highly significantly and negatively correlated with the MWD, GMD, and SOC ($P < 0.01$). Due to the vegetation restoration, the total organic carbon content of the soil increased. The organic carbon content of the soil in the woodland was significantly higher than those of the other types of vegetation. The organic carbon content of the soil in the bare land was the lowest of the various types of vegetation. The organic carbon contents of the WSA in the different types of vegetation varied significantly. As the soil particle size decreased, the organic carbon content increased. The organic carbon content of the aggregates < 0.25 mm was the highest, accounting for the majority of the total organic carbon content of the soil.

Acknowledgements. We gratefully acknowledge the editor and reviewers. This research was financially supported by the Fundamental Research Funds for the Central Non-profit Research Institution of CAF (CAFYBB2014ZD006). Thanks to S. Yan, G. J. Li and W. Zhou for their assistances with the fieldwork and lab measurements.

SED
6, 1–30, 2015

Title Page
Abstract Introduction
Conclusions References
Tables Figures
◂ ▸
Back Close
Full Screen / Esc
Printer-friendly Version
Interactive Discussion

References

Abu-Hamdeh, N. H., Abo-Qudais, S. A., and Othman, A. M.: Effect of soil aggregate size on infiltration and erosion characteristics, Eur. J. Soil Sci., 5, 609–616, 2005.

Bao, S. D.: Soil and Agricultural Chemistry Analysis, China Agriculture Press, Beijing, China, 2005.

Barral, M. T., Arias, M., and Guerif, J.: Effects of iron and organic matter on the porosity and structural stability of soil aggregates, Soil Till. Res., 3, 261–272, 1998.

Bryan, R. B.: Soil erodibility and processes of water erosion on hill slopes, Geomorphology, 32, 385–415, 2000.

Christensen, B. T.: Straw incorporation and soil organic matter in macro aggregates and particle size separates, Eur. J. Soil Sci., 37, 125–135, 1986.

De Jonge, L. W., Jacobsen, O. H., and Moldrup, P.: Soil water repellency effects of water content, temperature and particle size, Soil Sci. Soc. Am. J., 63, 437–444, 1999.

Dexter, A. R.: Advances in characterization of soil structure, Soil Till. Res., 11, 199–238, 1988.

Guo, W., Shi, Z. H., Chen, L. D., Li, C. X., Yan, L. F., and Cai, C. F.: Effects of topsoil aggregate size on runoff and erosion at hillslope in red soils, Acta Ecologica Sinica, 6, 2516–2522, 2007.

Hassink, J.: The capacity of soils top reserve organic C and N by their association with clay and silt particles, Plant Soil, 1, 77–87, 1997.

He, S. Q., Zheng, Z. C., and Gong, Y. B.: Distribution characteristics and soil organic carbon of soil water-stable aggregates with different de-farming patterns, J. Soil Water Conserv., 5, 229–233, 2011.

Jastrow, J. D.: Soil aggregates formation and the accrual of particulate and mineral-associated organic matter, Soil Biol. Biochem., 28, 656–676, 1996.

Jennifer, S. P.TS3: Changes in soil carbon and nitrogen after contrasting land-use transitions in Northeastern Costa Rica, Ecosystems, 7, 134–146, 2004.

Le Bissonnais, Y.: Aggregate stability and assessment of soil crushability and erodibility I: Theory and methodology, Eur. J. Soil Sci., 47, 425–435, 1996.

Le Bissonnais, Y. and Arrouays, D.: Aggregate stability and assessment of soil crustability and erodibility II: application to humic loamy soils with various organic carbon contents, Eur. J. Soil Sci., 48, 39–48, 1997.

Please note the remarks at the end of the manuscript.

Li, H. X., Yuan, Y. H., Huang, Q. R., Hu, F., and Pan, G. X.: Effects of fertilization on soil organic carbon distribution in various aggregates of red paddy soil, Acta Pedologica Sinica, 3, 422–428, 2006.

Li, J., Liao, H. K., Long, J., and Chen, C. Y.: Effect of land use on the characteristics of organic carbon and labile organic carbon in soil aggregates in Karst mountain areas, Acta Ecologica Sinica, 7, 2147–2156, 2013.

Li, L. Q., Pan, G. X., and Zhang, X. H.: Changes in organic carbon storage in aggregates of the surface horizon in a degraded Paleudlt upon vegetation recovery, Chinese Journal of Soil Science, 5, 193–195, 2000.

Liu, L., An, S. S., and Huang, H. W.: Application of Le Bissonnais method to study soil aggregate stability under different vegetation on the loess plateau, Acta Ecologica Sinica, 20, 6670–6680, 2013.

Liu, X. L. and He, Y. Q.: Water-stable aggregates and nutrients in red soil under different reclamation years, Soils, 1, 84–89, 2009.

Lu, L. X., Song, T. Q., Peng, W. X., Zeng, F. P., Wang, K. L., and Xu, Y. L.: Profile distribution of soil aggregates organic carbon in primary forests in Karst cluster-peak depression region, Chinese Journal of Applied Ecology, 5, 1167–1174, 2012.

Luo, Y. J., Wei, C. F., Li, Y., Ren, Z. J., and Liao, H. P.: Effects of land use on distribution and protection of organic carbon in soil aggregates in Karst rocky desertification area, Acta Ecologica Sinica, 1, 257–266, 2011.

Mao, Y. L., Yang, Y. S., Zou, S. Q., Chen, G. S., and Wang, G. Q.: Effects of land use on soil organic carbon in aggregates of hilly red soil in subtropical China, J. Mt. Sci., 6, 706–713, 2007.

Nimmo, J. R. and Perkins, K. S.: Aggregate stability and size distribution, in: Methods of Soil Analysis, Part 4: Physical Methods, edited by: Dane, J. H. and Topp, G. C., Soil Science Society of America, Madison, WI, USA, 317–328, 2002.

Novara, A., Rühl, J., La Mantia, T., Gristina, L., La Bella, S., and Tuttolomondo, T.: Litter contribution to soil organic carbon in the processes of agriculture abandon, Solid Earth, 6, 425–432, doi:10.5194/se-6-425-2015, 2015.

Pan, G. X. and Cao, J. H.: Karstification in Epikarst Zone: the Earth surface ecosystem processes taking soil as a medium – the Yaji Karst experiment site, Guilin, Carsologica Sinica, 4, 289–296, 1999.

Puget, P., Angers, D. A., and Chenu, C.: Nature of carbohydrates associated with water stable aggregates of two cultivated soils, Soil Biol. Biochem., 31, 55–63, 1998.
Puget, P., Chenu, C., and Balesdent, J.: Dynamics of soil organic matter associated with particle-size fractions of water-stable aggregates, Eur. J. Soil Sci., 51, 595–605, 2000.
Qi, Y. C., Wang, Y. Q., Liu, J., Yu, X. X., and Zhou, C. J.: Comparative study on composition of soil aggregates with different land use patterns and several kinds of soil aggregate stability index, T. ASAE, 1, 340–347, 2011.
Rachman, A., Anderson, S. H., and Gantzer, C. J.: Influence of long-term cropping systems on soil physical properties related to soil erodibility, Soil Sci. Soc. Am. J., 2, 637–644, 2003.
Sainju, U. M., Terrill, T. H., and Gelaye, S.: Soil aggregation and carbon and nitrogen pools under rhizoma peanut and perennial weeds, Soil Sci. Soc. Am. J., 67, 146–155, 2003.
Shi, H.: Using transition matrix to evaluate stability of soil aggregates, Bulletin of Soil and Water Conservation, 3, 91–95, 2006.
Tan, Q. J., Song, T. Q., Peng, W. X., Zeng, F. P., Du, H., and Yang, G. R.: Stability and organic carbon characteristics of soil aggregates under different ecosystems in karst canyon region, Chinese Journal of Applied Ecology, 3, 671–678, 2014.
Tang, F. K., Cui, M., Zhou, J. X., Yan, S., and Ding, F. J.: Difference analysis of soil organic carbon pool in different forestlands returned from farmlands in karst gorge area, Science of Soil and Water Conservation, 4, 1–7, 2014.
Tisdall, J. M. and Oades, J. M.: Organic matter and water-stable aggregates, J. Soil Sci., 33, 141–163, 1982.
Tyler, S. W. and Wheatcraft, S. W.: Application of fractal mathematics to soil water retention estimation, Soil Sci. Soc. Am. J., 53, 987–996, 1989.
Unger, P. W.: Aggregate and organic carbon concentration interrelationships of a Torrertic Paleustoll, Soil Till. Res., 42, 95–113, 1997.
Valmis, S., Dimoyiannis, D., and Danalatos, N. G.: Assessing interrill erosion rate from soil aggregate instability index, rainfall intensity and slope angle on cultivated soils in central Greece, Soil Till. Res., 80, 139–147, 2005.
Wei, Y. W., Su, Y. R., Chen, X. B., He, X. Y., Qin, W. G., and Wei, G. F.: Effects of human disturbance on soil aggregates content and their organic C stability in Karst regions, Chinese Journal of Applied Ecology, 4, 971–978, 2011.
Wu, J. G., Zhang, X. Q., and Xu, D. Y.: Impact of land use change on soil carbon storage, Chinese Journal of Applied Ecology, 4, 593–599, 2004.

Xiao, F. M., Fan, S. H., Wang, S. L., Xiong, C. Y., Yu, X. J., and Shen, Q. Z.: Mosbamboo plantation soil aggregate stability and its impact on carbon storage, Journal of Soil Water Conservation, 2, 131–134, 2008.
Yan, F. L., Shi, Z. H., Cai, C. F., and Li, C. X.: Effects of topsoil aggregate stability on soil erosion at hill slope on ultisoils, Acta Pedologica Sinica, 4, 577–583, 2007.
Yang, P. L., Luo, Y. P., and Shi, Y. C.: Fractal features characterized by soil particle size distribution of the weight, Chinese Sci. Bull., 20, 1896–1899, 1993.
Young, R. A.: Characteristics of eroded sediment, T. ASAE, 23, 1139–1146, 1980.
Yuan, D. X., Liu, Z. H., and Lin, Y. S.: Karst Dynamic System of China, Geological Publish Company, Beijing, China, 2002.
Zhang, X. B., Wang, S. J., and Cao, J. H.: Characteristics of water loss and soil erosion and some scientific problems on karst rocky desertification in Southwest China karst area, Carsologica Sinica, 3, 274–279, 2010.
Zhou, G., Zhao, H., Chen, G. Y., Xie, M. S., and Lai, Y. K.: Differential rule of soil anti-erodibility in different land-use of granite red soil region, Soil and Water Conservation in China, 9, 27–29, 2008.

SED
6, 1–30, 2015

Table 1. Basic properties of study plots.

Vegetation types	Altitude (m a.s.l.)	Slope (°)	Vegetation cover (%)	Dominant species	Land use
BL	696	20.2	< 10	*Imperata cylindrica*, *Arthraxon hispidus*	Farmland abandoned one year, with disturbancer of tillage and pasture
GL	710	22.1	70	*Imperata cylindrica*, *Leucas mollisima* and *Taraxacum mongolicum*	Natural secondary, with less human disturbance
SL	694	25.4	60	*Pyracantha fortuneana*, *Rosa cymosa* and *Dodonaea viscosa*	Natural secondary, with disturbance of pasture
WL	704	20.0	80	*Tona sinensis*, *Pteroceltis tatarinowii* and *Sapium sebiferum*	Natural secondary, with less human disturbance

SED
6, 1–30, 2015

SED
6, 1–30, 2015

A typical karst gorge region

F. K. Tang et al.

Table 2. The soil aggregate stability based on Саввинов method.

Vegetation types	Layer (cm)	$WSA_{>0.25}$ (%)	PAD (%)	MWD (mm)		GMD (mm)		*D*	
				Dry	Wet	Dry	Wet	Dry	Wet
BL	0–20	71.68Ab	21.5Cb	4.183Ad	1.588Ac	3.181Ac	0.699Ac	2.163Aa	2.649Ba
	20–40	68.21ABb	28.34Ba	4.085Ad	1.304ABc	2.627Bd	0.626Bc	2.192Aa	2.690ABa
	40–60	64.07Bb	31.87Aa	3.243Bd	1.169Bc	1.966Cd	0.535Cc	2.227Aa	2.725Aa
GL	0–20	83.36Aa	13.59Cc	5.335Ab	1.966Ab	3.882Ab	1.061Ab	2.037Aa	2.487Bc
	20–40	80.81Ba	16.33Bb	5.011ABb	1.642Bb	3.605ABb	0.913Ab	2.091Aa	2.505ABc
	40–60	74.31Ca	19.43Ac	4.883Bb	1.498Bb	3.384Bb	0.881Ab	2.121Aa	2.580Ac
SL	0–20	73.86Ab	23.13Ca	4.655Ac	1.697Ac	3.35Ac	0.71Ac	2.112Aa	2.603Ab
	20–40	68.69Bb	26.87Ba	4.467Ac	1.473ABbc	3.107ABc	0.638ABc	2.187Aa	2.623Ab
	40–60	66.5Bb	28.26Ab	4.415Ac	1.252Bc	2.842Bc	0.588Bc	2.224Aa	2.678Ab
WL	0–20	86.72Aa	10.68Bd	6.101Aa	3.618Aa	4.934Aa	1.981Aa	1.994Aa	2.425Bc
	20–40	81.03Ba	17.02Bb	5.882Aa	3.027Ba	4.534Ba	1.503Ba	2.045Aa	2.522ABc
	40–60	76.36Ca	21.1Ac	5.41Ba	2.505Ba	4.087Ca	1.151Ca	2.074Aa	2.556Ac

Note: different small letters in the same column meant significant differences in same layer of different vegetation types at 0.05 level, different capital letters in the same column meant significant differences in different soil layer of same vegetation types at 0.05 level, the same in the Table 3.

Table 3. Conservation ratio of aggregates and aggregate stability index.

Vegetation types	Layer (cm)	Conservation ratio of aggregates (%)						aggregate stability index (ASI)
		> 5 mm	5–2 mm	2–1 mm	1–0.5 mm	0.5–0.25 mm	< 0.25 mm	
BL	0–20	0.22	0.25	0.28	0.3	0.42	1	2.47Ab
	20–40	0.15	0.28	0.23	0.28	0.38	1	2.30Bb
	40–60	0.10	0.23	0.21	0.26	0.39	1	2.19Bb
GL	0–20	0.18	0.34	0.44	0.46	0.49	1	2.91Aa
	20–40	0.05	0.24	0.38	0.42	0.51	1	2.60Ba
	40–60	0.07	0.31	0.32	0.36	0.39	1	2.45Ba
SL	0–20	0.19	0.28	0.26	0.34	0.44	1	2.51Ab
	20–40	0.09	0.21	0.25	0.34	0.45	1	2.34Bb
	40–60	0.07	0.22	0.22	0.35	0.46	1	2.32Bb
WL	0–20	0.55	0.51	0.52	0.43	0.31	1	3.32Aa
	20–40	0.48	0.35	0.30	0.31	0.25	1	2.69Ba
	40–60	0.39	0.23	0.38	0.30	0.23	1	2.53Ba

SED
6, 1–30, 2015

A typical karst gorge region

F. K. Tang et al.

SED
6, 1–30, 2015

Table 4. Contribution rates of water stable aggregates organic carbon to SOC under different vegetation types (%, mean ± SE, $n = 3$).

Vegetation types	Layer (cm)	WSA sizes (%)					
		> 5 mm	5–2 mm	2–1 mm	1–0.5 mm	0.5–0.25 mm	< 0.25 mm
BL	0–20	5.38 ± 0.33d	17.68 ± 0.9bc	11.6 ± 1.27c	14.82 ± 1.08c	21.19 ± 0.19b	25.32 ± 0.46a
	20–40	4.92 ± 0.19d	13.92 ± 0.31c	12.65 ± 0.21c	16.42 ± 0.95b	16.78 ± 0.16b	27.88 ± 1.43a
	40–60	3.45 ± 0.20e	15.87 ± 1.05bc	13.6 ± 0.61c	10.49 ± 0.56d	19.78 ± 0.96b	41.08 ± 1.81a
GL	0–20	7.56 ± 0.21b	17.65 ± 0.57a	16.99 ± 0.38a	16.44 ± 0.45a	8.55 ± 0.23b	18.85 ± 0.35a
	20–40	2.43 ± 0.07d	18.45 ± 0.61b	22.37 ± 0.56a	18.57 ± 0.60b	11.26 ± 0.31c	24.10 ± 0.50a
	40–60	2.58 ± 0.15d	19.3 ± 0.95b	17.04 ± 0.6b	17.54 ± 0.57b	11.27 ± 0.34c	27.72 ± 0.73a
SL	0–20	4.24 ± 0.11d	9.84 ± 0.29c	9.28 ± 0.22c	9.11 ± 0.3c	11.71 ± 0.15b	26.51 ± 0.33a
	20–40	1.68 ± 0.10d	6.56 ± 0.41c	9.00 ± 0.34b	9.56 ± 0.46b	7.49 ± 0.40c	18.28 ± 0.65a
	40–60	1.26 ± 0.05d	7.85 ± 0.56c	11.26 ± 0.42b	12.44 ± 0.67b	11.42 ± 0.44b	32.18 ± 1.06a
WL	0–20	16.81 ± 0.19bc	17.29 ± 0.73b	14.66 ± 0.19c	9.39 ± 0.16d	5.49 ± 0.62e	22.19 ± 0.20a
	20–40	16.58 ± 0.19b	24.38 ± 0.78a	11.13 ± 0.21c	7.78 ± 0.54d	5.06 ± 0.11d	20.37 ± 0.36a
	40–60	13.91 ± 0.18b	24.99 ± 0.82a	16.25 ± 0.1b	9.95 ± 0.40c	6.43 ± 0.27d	26.91 ± 1.21a

Note: different small letters in the same row showed significant difference at 0.05 level among different sizes.

SED
6, 1–30, 2015

Table 5. Correlation between parameters of water stable aggregation.

		D	MWD	GMD	SOC	WSA sizes (mm)					
						> 5	5–2	2–1	1–0.5	0.5–0.25	< 0.25
D		1									
MWD		−0.544[b]	1								
GMD		−0.608[b]	0.963[b]	1							
SOC		−0.454[b]	0.701[b]	0.756[b]	1						
WSA sizes (mm)	> 5	−0.203	0.409[a]	0.265	0.588[b]	1					
	5–2	−0.346[a]	0.168	0.203	0.348[a]	0.798[b]	1				
	2–1	−0.202	0.224	0.121	0.418[a]	0.871[b]	0.808[b]	1			
	1–0.5	−0.215	0.194	0.172	0.410[a]	0.882[b]	0.817[b]	0.951[b]	1		
	0.5–0.25	0.312[a]	0.114	0.237	0.338[a]	0.822[b]	0.678[b]	0.947[b]	0.926[b]	1	
	< 0.25	0.633[b]	0.074	0.112	0.368[a]	0.865[b]	0.835[b]	0.960[b]	0.922[b]	0.951[b]	1

[a] $P < 0.05$; [b] $P < 0.01$.

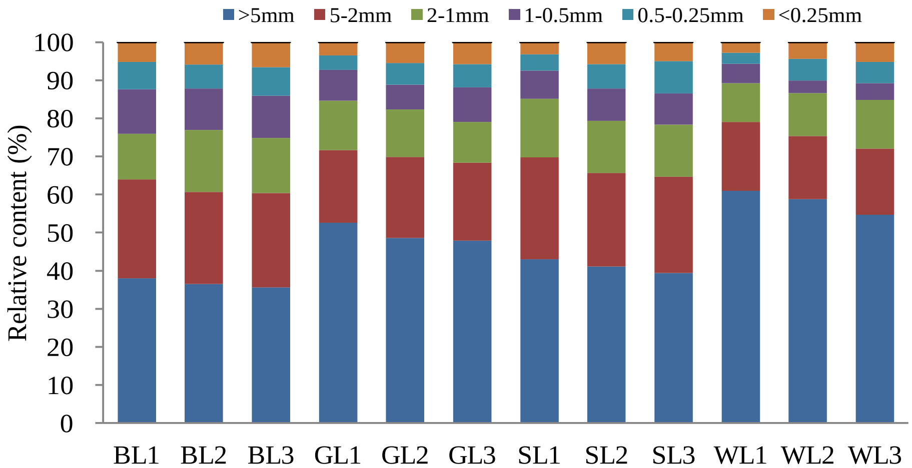

Figure 1. Relative distribution of soil dry-aggregates with different sizes under different vegetation types. (BL1, BL2, BL3, GL1, GL2, GL3, SL1, SL2, SL3, WL1, WL2, WL3 represent 0–20, 20–40, 40–60 cm soil layers for bareland, grassland, shrubland and woodland. The same in Figs. 2 and 3.)

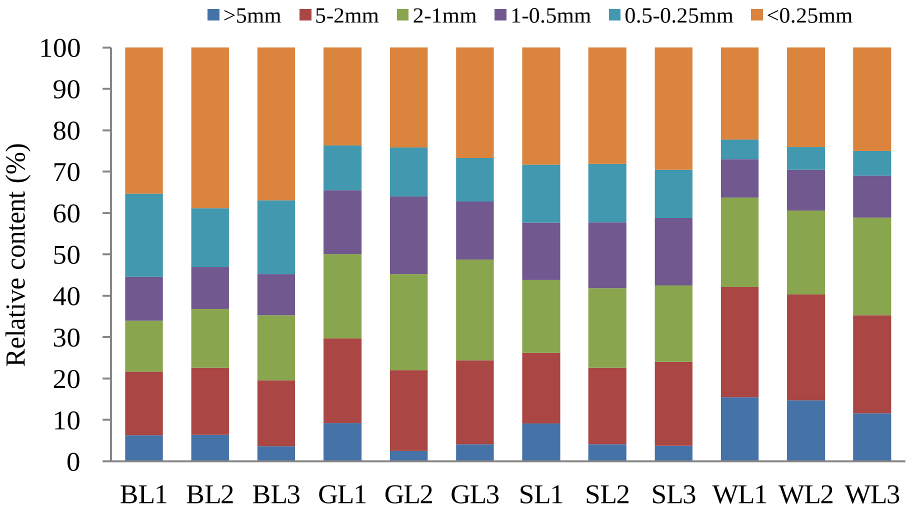

Figure 2. Relative distribution of soil water stable aggregates with different sizes under different vegetation types.

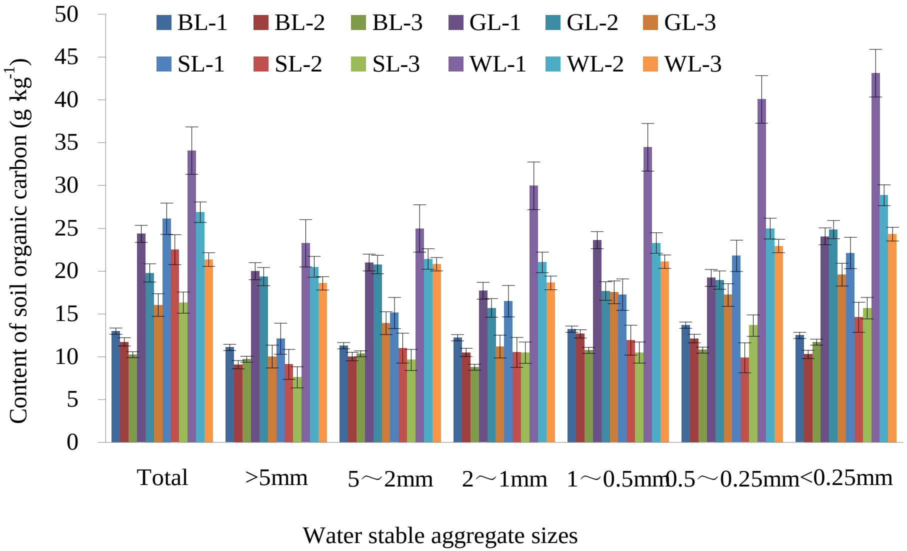

Figure 3. SOC in different water stable aggregate sizes under different vegetation types (mean ± SE, $n = 3$).

Remarks from the typesetter

TS1 Please check running title.
TS2 Please check through the whole text that all matrices are bold-roman and all vectors are bold-italic.
TS3 Please check. Do you mean Jennifer S. Powers?

SED
6, 1–30, 2015